THE JOURNAL OF PHYSICAL CHEMISTRY B

ARTICLE

pubs.acs.org/JPCB

# Probing the Role of Chain Length on the Diffusion Dynamics of π-Conjugated Polymers by Fluorescence Correlation Spectroscopy

A. V. R. Murthy,[†] Mahima Goel,[‡] Shivprasad Patil,*[,†] and M. Jayakannan*[,‡]

[†]Department of Physics and [‡]Department of Chemistry, Indian Institute of Science Education and Research (IISER)-Pune, Dr. Homi Bhabha Road, Pune 411008, Maharashtra, India

Supporting Information

**ABSTRACT:** We investigate the role of the chain length and molecular weight distribution on the diffusion dynamics of freshly synthesized MEH-PPV polymer chains. For the above purpose, a new technique based on combination of size exclusion chromatography (SEC) with fluorescence correlation spectroscopy (FCS) is developed to probe the diffusion dynamics of a narrow molecular weight distribution of fractionated samples of 20−500 kDa. The narrow dispersed samples were characterized by absorbance, emission, and time-resolved fluorescence decay techniques. The results revealed that the properties of fractionated samples were almost uniform for a wide range of molecular weights. A maximum entropy based method for FCS data analysis is employed to obtain the correct diffusion coefficients of the polymer chains with heterogeneous dynamics. The FCS experiment on the unfractionated broad molecular weight sample is not enough to establish the correlation between the molecular weight of the chains with diffusion dynamics and emphasized the need for relatively monodispersed π-conjugated polymers. FCS results show that higher molecular weight chains diffuse much faster than shorter ones. Atomic force microscopy revealed that 300 kDa polymers produced 130 nm particles, whereas 50 kDa polymer chains formed micrometer size aggregates. At higher molecular weights, the strong chain interactions promote the formation of globular (or tightly packed) particles which diffuse faster in solution. The low molecular weight chains experience strong interparticle interaction; as a consequence, the diffusion of chains becomes slower. In the present investigation, we demonstrate the need for the narrow polydisperse sample for establishing the correlation between diffusion dynamics and chain length (or molecular weights) of π-conjugated polymers using a single molecule spectroscopy technique such as FCS.

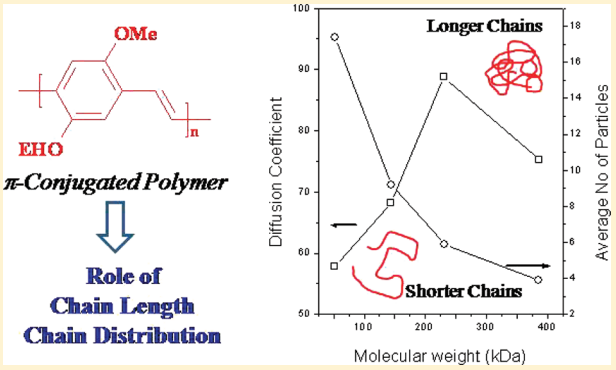


## INTRODUCTION

Conjugated polymers are emerging as an important class of materials due to their potential applications in electronic devices such as light emitting diodes, photovoltaics, and field effect transistors.[1−4] In general, π-conjugated polymers have a very strong tendency for aromatic π- stacking via inter- or intrachain interactions, which leads to the formation of micrometer- to subnanometer-sized aggregated species.[5−8] These molecular aggregates typically exist as low energy nonemissive species in which the excitation energy of the highly luminescent excimers gets trapped during the radiative decay. As a consequence, highly emissive polymers show low quantum efficiency or unwanted emission from aggregated species in solutions or in the solid state (in films). Recently, there has been a significant effort to understand the formation of this π-stack induced molecular aggregation in the highly emissive π-conjugated polymers.[9−12] A few synthetic approaches such as confinement of conjugation via cis-vinylene linkages[13−18] or separation of polymer chains through the introduction of bulky anchoring groups[19−23] were developed to address the aggregation phenomenon. Among the various conjugated polymers, poly(*p*-phenylenevinylene) (PPV) based polymers such as poly(2-methoxy-5(2-ethylhexyl)-1,4-phylene-vinylene) (MEH-PPV) is one of the most thoroughly studied electroluminescent polymers.[24] MEH-PPV structure is very unique in the sense that the branched ethylhexyloxy unit enhances the solubility of the polymer chain in common solvents and also shows improved luminescence properties by reducing molecular aggregation via the branched chain. In our efforts to understand the aggregation in conjugated chains, we reported new bulky PPV homopolymers,[25] random copolymers,[26,27] and bulky oligophenylenevinylenes[28,29] based on tricyclodecane-methanol. The role of solvent polarity, annealing temperature, and molecular weight on the chain aggregation properties of the MEH-PPV were also reported.[30] Though these photophysical techniques provide some insight into the bulk properties of the polymers in solution or in film, it is very difficult to rationalize the role of polymer chain length on the molecular aggregation. Fluorescence correlation spectroscopy (FCS) is emerging as a

**Received:** April 29, 2011
**Revised:** August 12, 2011
**Published:** August 15, 2011

ACS Publications © 2011 American Chemical Society



dx.doi.org/10.1021/jp203978v | *J. Phys. Chem. B* 2011, 115, 10779–10788

powerful single molecule technique to trace the diffusion dynamics of a single or few polymer chains in extreme dilution at nanomolar concentrations.[31] FCS determines the rate kinetics as well as the diffusion dynamics using minute fluctuations in the intensity at thermal equilibrium.[32,33] Such deviations occur due to both the motion of particles or chains as well as inter- or intramolecular chemical interactions. It is straightforward to measure the local concentrations, diffusion coefficients, and rate kinetics of molecular interactions using FCS. Recently, Lin et al.[34] and Summers et al.[35] independently reported the fluorescence characteristics of a single molecule of commercially available MEH-PPV polymers (molecular weights of 37 and 1400 kDa) and tetrahedral phenylenevinylene oligomers using FCS. In both cases, nonfluorescent conjugated polymers like poly(methylmethacrylate) (PMMA) or polystyrene were used to optimize or facilitate the uniform diffusion of conjugated chains in solution. Though the fluorescent decay dynamics of pure MEH-PPV chains were found comparable to that of the MEH-PPV/PMMA blends, a large difference in the collapsing of the chain conformations was noticed. The difference in the conformational change of the $\pi$-conjugated chains in association with PMMA chains was attributed to the presence of the nonemissive PMMA (or polystyrene) as a dark matter. This limits the understanding of the diffusion properties of pure $\pi$-conjugated chains in solution. Investigating the diffusion dynamics of $\pi$-conjugated chains is very important because it will provide more insight into the interchain interaction for processing these materials in electronic devices. To our knowledge, there has not been a systematic effort to study the influence of chain length and molecular weight distribution on the diffusion dynamics of $\pi$-conjugated polymers at the single molecular or chain level. Therefore, it is very important to develop new approaches for conjugated polymers alone (without blending with other nonemissive polymers such as PMMA or polystyrene) to study their solution dynamics by a single molecule technique such as FCS.

The emphasis of the present investigation is to address the above problem by combining FCS with the size exclusion chromatography (SEC) technique in freshly synthesized MEH-PPV polymers. It is also aimed to address the following important fundamental questions: (i) What are the effects of the chain length (or molecular weight) and the narrow molecular weight distribution on the diffusion dynamics of the $\pi$-conjugated chains? (ii) What is the effect of molecular weight on the interchain interactions of conjugated polymers? (iii) What is the effect of external stimuli such as temperature and concentration on the diffusion dynamics of polymer chains? For this purpose, freshly synthesized MEH-PPV polymer was fractionated to obtain narrow molecular weight fractions of varying molecular weights ranging from 20 to 500 kDa. The samples were characterized by NMR, FT-IR, absorbance, emission, and time-resolved fluorescence decay techniques to understand the effect of molecular weight on photophysical properties. Additionally, we used FCS and the maximum entropy based method for FCS data analysis (MEMFCS) to trace the polymer chain interactions through diffusion dynamics at the single molecule level. FCS analysis of the narrow fractionated samples revealed that their diffusion dynamics is highly dependent on the chain length (or molecular weight) and distribution. The diffusion coefficients of long polymer chains were found to be much higher compared to those of the shorter ones. Atomic force microscopy (AFM) imaging was also carried out to investigate the nature and size of the aggregates produced by these chains from dilute solutions. The average number of chromophores in the detection volume was found to be more for shorter chains compared to that of the longer ones. The size of the polymer chains and intermolecular interactions play major roles in the diffusion dynamics in solution. This clearly shows that the development of the SEC fractionation technique in combination with FCS provides a new opportunity to investigate the role of chain length and molecular weight distribution on the aggregation behavior of $\pi$-conjugated polymers.

## EXPERIMENTAL SECTION

**Materials.** 4-Methoxyphenol, 2-ethylhexylbromide, potassium-*t*-butoxide (1 M in THF), and rhodamine 6G were purchased from Aldrich Chemicals. HBr in glacial acetic acid, paraformaldehyde, and KOH were purchased locally. Solvents were also purchased locally and were purified by standard procedures.

**General Procedures.** $^1$H and $^{13}$C NMR spectra were recorded using a 400 MHz JEOL NMR spectrometer. All NMR spectra were recorded in $CDCl_3$ containing TMS as the internal standard. Infrared spectra were recorded using a Thermo-Scientific Nicolet 6700 FT-IR instrument in solid state in KBr. For the photophysical studies, all the solvents were purified according to the purification procedures prior to use. The polymer samples were completely dissolved by heating, and the homogeneous solutions thus obtained were used for further studies. The absorption spectra were recorded by a Perkin-Elmer Lambda 45 UV−visible spectrophotometer. The emission studies were done using a Florolog HORIBA JOBIN VYON fluorescence spectrophotometer with a 450 W Xe lamp as the excitation source using the reverse face mode. The quantum yields of polymer samples were determined using rhodamine 6G in water ($\phi$ = 0.95). TCSPC fluorescence lifetime measurements were done by using a HORIBA JOBIN YVON Nano-LED source with a 460 nm wavelength to excite all the samples, and emission was collected at 560 nm. Fluorescence lifetime values were determined by deconvoluting the data with exponential decay using DAS6 decay analysis software. The quality of fit was judged by fitting parameters such as $\chi^2 \approx 1$, as well as the visual inspection of the residuals. The molecular weight determination and fractionation of MEH-PPV was done by the size exclusion chromatography (SEC) (or gel permeation chromatography, GPC) technique. A Viscotek GPC setup with mixed bed columns was utilized, and the signals were detected using RI, UV, and light scattering detectors. HPLC grade tetrahydrofuran was employed as a solvent for the samples, and the GPC setup was calibrated with polystyrene standards. An atomic force microscope from JPK instruments, Nanowizard III, was used for imaging the MEHPPV aggregates on the mica substrate. The sample was prepared by the drop-cast method on mica substrates. The cantilevers from budget sensors having a stiffness of 40 N/m were used, and the imaging was performed in tapping mode.

**Synthesis of 1-(2-Ethylhexyloxy)-4-methoxybenzene.** 4-Methoxyphenol (9.92 g, 0.08 mol) and KOH (8.96 g, 0.16 mol) were taken in DMSO (200 mL), and the mixture was refluxed at 80 °C for 2 h. Ethylhexylbromide (22.6 mL, 0.12 mol) was added dropwise to the reaction mixture, and it was refluxed for 24 h. It was poured in 500 mL of water, extracted in dichloromethane, washed with 5% NaOH, brine solution, and dried over anhydrous sodium sulfate. The solvent was removed to obtain the product as a brown colored solid. It was purified by passing though a silica gel column using 0.5% ethyl acetate in hexane as eluent. Yield = 9.4 g

(49%). $^1$H NMR ($CDCl_3$, 400 MHz) $\delta$: 6.8 ppm (s, 4H, Ar-**H**); 3.7 ppm (dd, 2H, $-OC\mathbf{H_2}-CH$), 3.7 (s, 3H, $OC\mathbf{H_3}$), 1.4 (m, 1H, $OCH_2-C\mathbf{H}$), 1.4−0.9 ppm (m, 14H, alkyl). $^{13}$C NMR ($CDCl_3$,100 MHz) $\delta$: 153.5, 153.5, 115.3, 114.5 (Ar−**C**), 71.08 ($Ar-O\mathbf{C}H_2$), 55.7, 39.4, 30.8, 29.1, 23.8, 23, 14.1, and 11.05 ppm. FT-IR (KBr, $cm^{-1}$): 2936.8, 2361.2, 2066.9, 1596.8, 1510.2, 1465.2, 1384.1, 1108.4, 1037, 821.2, 742.1, and 521.5.

**Synthesis of 1,4-Bis(bromomethyl)-2-(2-ethylhexyloxy)-5-methoxybenzene.** 1-(2-Ethylhexyloxy)-4-methoxybenzene (2.36 g, 0.01 mol) and *p*-HCHO (1.20 g, 0.04 mol) were taken in 30 mL of glacial acetic acid. HBr in glacial acetic acid (5.0 mL, 0.01 mol) was added using a pressure equalizing funnel. The reaction mixture was refluxed for 8 h and cooled to room temperature, and the contents were then poured into a large amount of water. The product precipitated as a white solid, and the filtered solid was crystallized from hot acetone. Yield = 2.7 g (95%). Mp = 82 °C.[36] H NMR ($CDCl_3$, 400 MHz) $\delta$: 6.8 ppm (s, 2H, Ar−**H**), 4.5 ppm (s, 4H, $-C\mathbf{H_2}Br$), 3.8 ppm (s, 3H, $-OC\mathbf{H_3}$), 3.8 ppm (dd, 2H, $OC\mathbf{H_2}-CH$), 1.5−0.8 ppm (m, 15H, aliphatic-H). $^{13}$C NMR ($CDCl_3$, 100 MHz) $\delta$: 150.9, 150.9, 127.4, 127.2, 114.2, 113.7 (Ar−**C**), 70.8 ($Ar-O\mathbf{C}H_2-CH$), 56.2, 39.5, 29.0, 28.6, 23.9, 23.2, 14.0, and 11.2 ppm (aliphatic-C). FT-IR (KBr, $cm^{-1}$): 2933.3, 2871.6, 1726.4, 1513.1, 1459.9, 1400.9, 1312.7, 1106.4, 1033.6, 871.6, 675.0, 542.4, and 446.1.

**Synthesis of MEH-PPV.** 1,4-Bis(bromomethyl)-2-(2-ethylhexyloxy)-5-methoxybenzene (0.84 g, 2.0 mmol) was dissolved in dry THF (80 mL), and the reaction mixture was cooled to 5 °C. Potassium *tert*-butoxide (12.0 mL, 1 M THF solution) was added dropwise to the reaction mixture under nitrogen atmosphere. It was stirred at 30 °C for 24 h, and the resultant orange-red solution was poured into a large amount of methanol. The red precipitated polymer was dissolved in THF and reprecipitated again in methanol. The polymer was dried in a vacuum oven overnight. Yield: 0.2 g (38%). $^1$H NMR ($CDCl_3$, 400 MHz) $\delta$: 7.5 ppm (b, 2H, Ar−**H**), 7.1 ppm (s, 2H, $C\mathbf{H}{=}C\mathbf{H}$), 3.9 ppm (m, 5H, $OC\mathbf{H_3}$ and $-OC\mathbf{H_2}-$), 1.8−0.8 ppm (m, 15H, aliphatic). FT-IR (KBr, $cm^{-1}$): 3757.2, 3447.6, 2936.4, 2860.6, 2364.1, 2152.6, 1712.4, 1632.9, 1508.5, 1462.6, 1411.1, 1351.9, 1039.02, 968.9, 863.7, and 722.1.

**FCS Instrumental Setup.** A home-built fluorescence correlation spectroscope was used to measure the diffusion dynamics of all the fractionated polymer chains (see the Supporting Information). A DPSS laser (532 nm, 15 mW from Dream lasers, China) was used as an excitation source along with a neutral density filter to reduce the power by 50%. The laser beam was expanded and collimated to 10 mm using a combination of lenses having a focal length of 20 and 2.4 cm. A water immersion objective (1.2 NA, 60× from Olympus, Japan) was used to focus the light. The fluorescence collected from the objective was separated from the excitation light using a dichroic filter (560DCLP, omega optics, USA) and was further filtered using an emission filter. The light from the filter passes through a 15 cm achromatic lens (Thorlabs, USA) into a multimode fiber (25 $\mu$m inner diameter, OZ optics Canada) coupled to a single photon counting module (Perkin-Elmer Optoelectronics, Canada). A correlator card (Flex99oem-12D, correlator.com, USA) was used to calculate the autocorrelation of the intensities.[37] The MEMFCS algorithm developed at the School of Chemical Sciences, Tata Institute of Fundamental Research, Mumbai, was used for the fitting procedure. A temperature cell was designed around the sample holder (glass vial) that could reach up to 80 °C. The detection volume dimensions are as follows: the radius of the beam waist $r$ = 0.24 $\mu$m and length $l$ = 2.4 $\mu$m. A band pass filter was used for the 550−650 nm wavelength with 80% transmission. The projected pinhole in our measurement is 20 $\mu$m, and the fiber core diameter is 25 $\mu$m.

**Fluorescence Correlation Spectroscopy and Maximum Entropy Method.** The fluorescence fluctuations were measured over a period much longer than the diffusion time scales of the polymer chains in solution. The autocorrelation of these fluctuations was computed in the following manner.

$$G(\tau) = \frac{\langle \delta F(t)\, \delta F(t+\tau)\rangle}{\langle F(t)\rangle^2} \tag{1}$$

This is the measured autocorrelation for single diffusing species in three-dimensional excitation, where $G(\tau)$ is the measured autocorrelation, $\delta F(t)$ is the intensity fluctuation at time $t$, $\delta F(t+\tau)$ is the intensity fluctuation at time $(t+\tau)$, and $F(t)$ is the average fluorescence intensity. This is fitted with the equation

$$G(\tau) = \frac{1}{N}\left(\frac{1}{1+(\tau/\tau_D)}\right)\left(\frac{1}{1+(r/l)^2(\tau/\tau_D)}\right)^{1/2} \tag{2}$$

where $N$ is the average number of molecules in the detection volume: $\tau$ is the lag time, $\tau_D$ is the residential time, and $r/l$ is the structure parameter related to the geometry of the detection volume. This is a ratio of the radius of the beam waist and the axial length. For fickian diffusion, the diffusion time, average time spent by the fluorophore in the detection volume, is related to the diffusion coefficient with the equation

$$D = \frac{r^2}{4\tau_D} \tag{3}$$

Finally, the hydrodynamic radius $R_H$ is related to the diffusion coefficient by the Stokes−Einstein relationship.

$$D = \frac{kT}{6\pi\eta R_H} \tag{4}$$

where $k$ is the Boltzmann constant, $T$ is the absolute temperature, $R_H$ is the hydrodynamic radius, and $\eta$ is the viscosity of the medium.

The above-mentioned procedure works well for single component diffusion. For more than one diffusing species having different hydrodynamic radii, we need to fit the following equation:

$$G(\tau) = \sum_{i=1}^{n} \alpha_i \left(\frac{1}{1+(\tau/\tau_{Di})}\right)\left(\frac{1}{1+(r/l)^2(\tau/\tau_{Di})}\right)^{1/2} \tag{5}$$

where the index $i$ represents the number of diffusing species and $\alpha_i$ is the amplitude of the $i$th species. The above equation fits well for single, two, as well as three component diffusion but ceases to operate successfully as the number of diffusing species increases further and the goodness of the fit is difficult to determine. Long chain polymers are more likely to have a distribution of diffusing species than single component diffusion. All the previous FCS studies on such polymers used a single component diffusion fitting for determining the hydrodynamic radius of the polymer chains. However, it is more likely that these polymers in dilute conditions could be in different stages of folding, rendering their diffusivity to be heterogeneous. Hence, a simple fit to eq 2 may

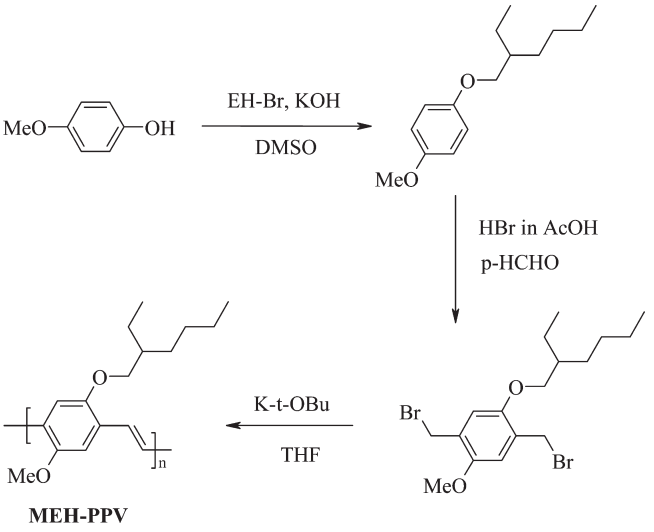


**Figure 1.** Synthesis of MEH-PPV polymer.

lead to an incorrect interpretation of the data. To take care of these issues, a method developed by Sengupta et al.[38] to determine the distribution of diffusion coefficients for heterogeneous dynamics was employed. This method known as the maximum entropy based method for FCS data analysis (MEMFCS) is a bias-free model independent method of fitting that can work for quasi-continuous distribution of diffusing components. This algorithm takes equal values for all the $\alpha_i$'s and $\tau_{Di}$'s and seeks a distribution where entropy is maximized and $\chi^2$ is minimized which estimates the goodness of the fit. For more details on this fitting procedure, see Sengupta et al.[38]

## RESULTS AND DISCUSSION

Poly[2-methoxy-5-(2-ethylhexyloxy)-1,4-phenylenevinylene] (MEH-PPV) was synthesized by the Gilch route from bis-bromomethylated monomer using potassium *tert*-butoxide as base catalyst at 30 °C in THF, as shown in Figure 1.[25,26] The structures of polymers and monomers were confirmed by NMR and FT-IR spectroscopy, and the details are given in the Supporting Information. The $^1$H NMR spectrum of MEH-PPV polymer showed two broad peaks at 7.4 and 7.1 ppm corresponding to phenyl aromatic protons and vinylene protons, respectively. The peaks for all other protons appeared below 4.00 ppm, and the intensities of all the protons matched with that of the expected structure. The molecular weight of the synthesized polymer was determined by SEC. SEC chromatograms are given in Figure 2, and molecular weights are given in Table 1. The synthesized sample showed a broad distribution (see Figure 2a) with $M_n$ = 38 700 and $M_w$ = 183 000 with a polydispersity of 4.7. The broad SEC chromatogram showed a large elution time from 12 to 18 min (see Figure 2a). This provides the opportunity to fractionate the sample into narrow dispersed fractions. About 100 $\mu$L of 0.5 mg/mL of the sample in THF was injected into the SEC column, and the samples were collected every 30 s after 12 min of the elution time. A total of 10 fractions were collected, and the process was repeated at least 10 times to collect more amounts of the samples in each fraction. The fractionated samples were concentrated and injected again for the determination of their respective molecular weights. The chromatograms for each of the fractions are shown in Figure 2b, and their

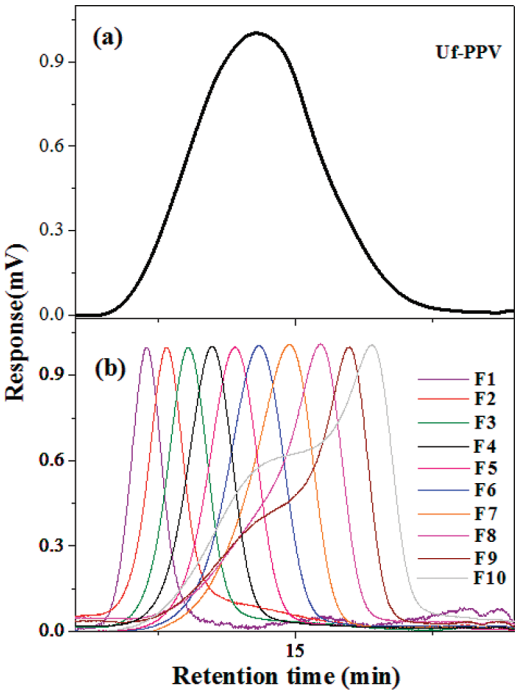


**Figure 2.** SEC chromatograms of **uf-PPV** and fractionated samples.

molecular weights are summarized in Table 1. Hereafter, the unfractionated MEH-PPV sample is referred to as **uf-PPV** and all fractionated samples are referred as **F*n*** where "***n***" represents the SEC fraction number. In Figure 2b, the SEC chromatograms of the fractionated samples are very well separated from each fraction. This suggests that the technique adopted here is very robust to isolate MEH-PPV samples with various molecular weights ranging from $M_n$ = 500 to 20 kDa (see Table 1). The fractions **F1**, **F9**, and **F10** were obtained in very small quantities, and they were not used for any further analysis. It is very important to mention that the molecular weights of the polymers are determined with respect to polystyrene standards (used for calibration of SEC), and therefore, the molecular weights of the fractions may be little overestimated. This has arisen because of the difference in the hydrodynamic volume of the polystyrene standards with that of MEH-PPV in THF. Hence, the polydispersity of the samples calculated on the basis of $M_w/M_n$ values may be little different from the actual distribution of the chains. The full width at half-maximum of the retention time ($R_{fwhm}$, $R$ = retention time) of the SEC chromatogram is another important quantity which directly provides the distribution of the polymer chains in fractionated samples irrespective of the standards used for calibration of the SEC. The $R_{fwhm}$ values for all the fractions were determined, and the data are provided in Table 1. For instance, the narrow dispersed sample (**F2**) has lower $R_{fwhm}$ compared to that of its broad molecular weight counterpart (**F8**). The $M_n$, $M_w$, polydispersity, and $R_{fwhm}$ values are plotted for each fraction and shown in the Supporting Information (see Figure 3 in the Supporting Information). Both $M_n$ and $M_w$ molecular weights followed a linear trend, indicating that the SEC fractionation methodology adopted in the present approach was very effective in separating different chain lengths. It is clearly evident that the fractionated samples are found to show narrow distribution as compared to that of the unfractionated sample (**uf-PPV**). The polydispersity data (see table 1) shows a nonlinear trend and

**Table 1. Molecular Weights and Photophysical Properties of Polymer Samples**

| sample[a] | $M_n$[b] | $M_w$[b] | $M_w/M_n$ | $R_{fwhm}$[c] (s) | $\lambda_{max}$(Abs)[d] (nm) | $\lambda_{max}$(Em)[e] (nm) | $\Phi$[f] | $\tau_1$[g] (ns) | $\tau_2$[g] (ns) |
|---|---|---|---|---|---|---|---|---|---|
| **Uf-PPV** | 38700 | 183000 | 4.7 | 158 | 498 | 556 | 0.22 | 0.32 | 1.61 |
| **F2** | 524000 | 688000 | 1.3 | 46 | 490 | 554 | 0.24 | 0.34 | 1.76 |
| **F3** | 386000 | 467000 | 1.2 | 50 | 489 | 552 | 0.25 | 0.38 | 1.48 |
| **F4** | 231000 | 307000 | 1.3 | 55 | 487 | 552 | 0.25 | 0.34 | 1.29 |
| **F5** | 144000 | 198000 | 1.3 | 61 | 490 | 551 | 0.24 | 0.34 | 1.34 |
| **F6** | 86000 | 129000 | 1.5 | 69 | 491 | 554 | 0.24 | 0.33 | 1.73 |
| **F7** | 52000 | 90000 | 1.7 | 76 | 490 | 553 | 0.25 | 0.33 | 1.31 |
| **F8** | 31600 | 73000 | 2.3 | 80 | 489 | 553 | 0.24 | 0.34 | 1.57 |

[a] Fractions **F1**, **F9**, and **F10** were obtained in small quantities and not used for further analysis; their molecular weights are given in the Supporting Information. [b] Number average ($M_n$) and weight average ($M_w$) molecular weights are determined by the SEC technique using polystyrene standards at 30 °C. [c] $R_{fwhm}$ is the full width at half-maximum for the retention time based on SEC chromatograms. [d] Absorption maxima, $\lambda_{max}$(Abs), were obtained in toluene. [e] Emission maxima, $\lambda_{max}$(Em), were recorded using 0.1 OD solutions in toluene and by exciting the sample at 490 nm. [f] Quantum yields ($\Phi$) of the polymers in solution were determined using rhodamine 6G as a standard. [g] Fluorescence lifetimes ($\tau_1$ and $\tau_2$) of 0.1 OD solutions were determined by the TCSPC method using 460 nm Nano-LED sources. Data were fitted with a biexponential decay curve with $\chi^2 \cong 1.02-1.07$.

the values are almost invariant up to **F5** and appeared little broad from **F6** to **F8**. The plot of $R_{fwhm}$ versus the fraction number showed linear trend for the entire molecular weight samples which indicates that $R_{fwhm}$ is a better data to represent the dispersity of the fractionated samples rather than $M_w/M_n$ (see Figure 3, in the Supporting Information). Though all chromatograms are monodisperse (for **F2**−**F8**, see Figure 2b), the $R_{fwhm}$ values increase with a decrease in the molecular weights (toward low fraction number). It indicates that the polydispersity of the fractionated samples increases with a decrease in the molecular weights. It may be summarized that all the fractionated samples are monodispersed; however, they vary in their chain length (or molecular weight) as well as distribution. This facilitates the investigation on the role of polymer chain length (also distribution) in the diffusion kinetics and luminescent characteristics on a wide range of narrow distributed MEH-PPV samples.

The photophysical properties of the fractionated samples were studied in toluene. Toluene was chosen as the solvent for spectroscopic studies, since it has a high boiling point, has a low vapor pressure, and is not hygroscopic under atmospheric conditions. Further, toluene is found to be a suitable solvent for studying chain interactions in conjugated polymers, more specifically MEH-PPVs.[30] For this purpose, fractionated samples were completely dried and then redissolved in HPLC grade toluene. The molar extinction coefficient of MEH-PPV was determined as $1.9 \times 10^4$ L mol$^{-1}$ cm$^{-1}$, and it is used for determination of the concentration of polymer samples employed for photophysical studies. Polymer solutions (in toluene) with an optical density of 0.1 (concentration = $5.3 \times 10^{-6}$ M) were prepared for photophysical studies. The absorption and emission spectra of the **F2**−**F8** and **uf-PPV** samples are shown in Figure 3a and b, respectively (see Table 1 for photophysical data). The emission spectra were recorded by exciting at 490 nm, and rhodamine 6G was used as a standard to determine the quantum yield of the samples. The quantum yields of the polymers in solution were determined using the following equation: $\phi_s = \phi_r(F_sA_r/F_rA_s)(n_s/n_r)^2$, where $\phi_s$ is the fluorescent quantum yield, $F$ is the area of the emission curve, $n$ is the refractive index of the solvent, and $A$ is the absorbance of the solution at the exciting wavelength. The subscripts r and s denote the reference and sample, respectively. The absorbance, emission maxima, and quantum yield of the fractions are plotted against $M_n$ and are shown in the Supporting Information (see Figure 4 in the Supporting Information). The unfractionated sample, **uf-PPV**, has absorbance maxima at 498 nm which is almost 10 nm red-shifted compared to that of the fractionated samples (see Table 1). The red shift in the unfractionated sample indicates that the sample has more aromatic $\pi$-stacking in solution through strong polymer chain interactions. Interestingly, the photophysical properties and quantum yields of the fractionated samples were almost uniform for a wide range of molecular weights ranging from 500 to 32 kDa. The quantum yield of the samples was obtained in the range 0.22−0.25, which are in accordance with earlier reports for

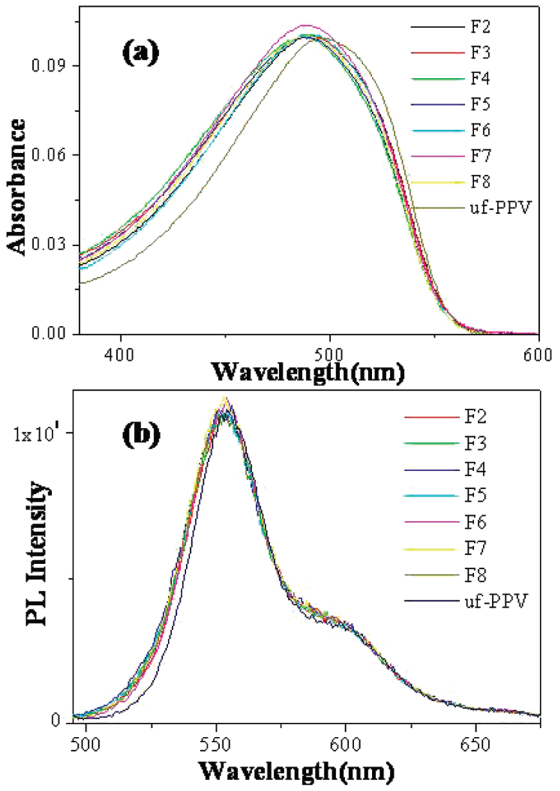


**Figure 3.** Absorbance (a) and emission (b) spectra of the polymer fractions in toluene at 30 °C. The emission spectra were recorded by exciting at 490 nm.


dx.doi.org/10.1021/jp203978v |J. Phys. Chem. B 2011, 115, 10779–10788

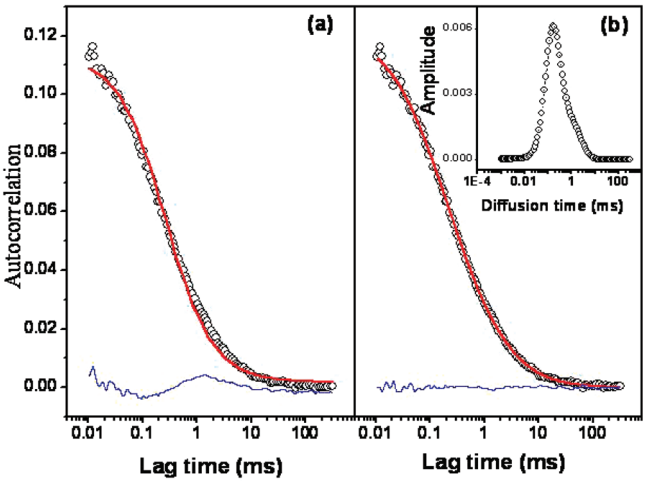


**Figure 4.** Autocorrelation data of fraction **F5** fitted with conventional single component fit (a) and MEMFCS fit (b). The inset shows the distribution of diffusion time.

MEH-PPV samples.[39,40] Further, time-resolved fluorescence decay measurements were performed using the TCSPC setup. For this purpose, 0.1 OD (optical density) solution of each fraction in toluene was excited with 460 nm Nano-LED sources and the emitted light was collected at 560 nm. The data were fitted with a biexponential fit, and the values are summarized in Table 1. The $\tau_1$ and $\tau_2$ values were obtained in the range 0.32−0.38 and 1.30−1.70 ns, respectively. The fluorescence decay values for the samples were almost the same and are in accordance with the literature reports.[40] The photophysical characteristics of polymer chains were almost identical in all fractionated samples irrespective of their difference in molecular weights and distribution. The above analysis confirmed that the narrow dispersed samples produced by SEC fractionation are very much suitable for further understanding their diffusion dynamics in dilute solutions using single molecule techniques such as FCS.

FCS is a single molecule technique that determines the kinetics as well as the diffusion dynamics using minute fluctuations in the intensity at thermal equilibrium. Such deviations occur both due to the motion of particles or chains as well as inter- or intramolecular chemical interactions. Since the dynamics of the polymer chains is expected to be heterogeneous with a distribution of diffusion time scales, it becomes necessary to use the MEMFCS fitting algorithm to obtain the correct diffusion coefficients of the polymer chains.[37,38] The autocorrelation curve for 144 kDa (for **F5**) for a measurement time of 100 s is shown in Figure 4. The data was fitted using a conventional single component fit (see Figure 4a) as well as the MEMFCS fitting algorithm (see Figure 4b). It is clearly evident that the MEMFCS algorithm shows better fitting with less residue compared to that of the conventional fitting.[37] The diffusion coefficient (eq 3) determined from the MEMFCS fit (the peak in the distribution) is 85.2 $\mu m^2/s$ with a fwhm of 30.1 $\mu m^2/s$, whereas the diffusion coefficient obtained from a single component fit is 52.7 $\mu m^2/s$. This suggests that the heterogeneous distribution is present in the diffusion of the chains and hence the MEMFCS fitting procedure is more suitable to study polymer chain dynamics. Hence, in the present work, the MEMFCS fitting is used for FCS data analysis. To optimize the experimental

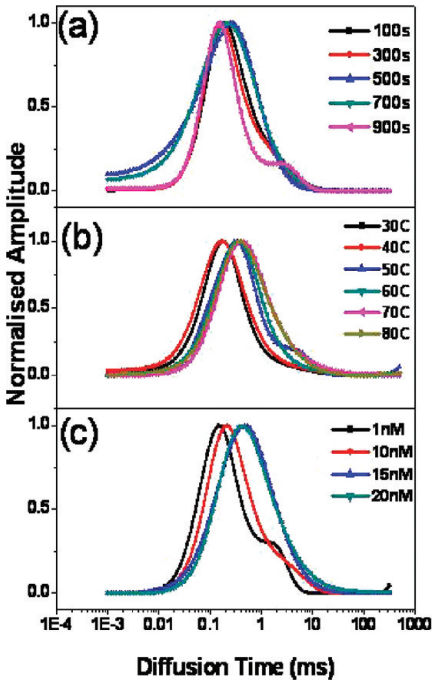


**Figure 5.** MEMFCS fits for fraction **F5** at various times (a), temperatures (b), and concentrations (c).

conditions for measurement of diffusion dynamics of MEHPPV chains in toluene, we performed experiments to establish the optimum parameters such as measurement time, temperature, and concentration of chain chromophores. The experiments were performed at regular time intervals of 200 s (time $t = 0$ is corresponding to the initial exposure of laser source) to establish the stability of the luminescent chromophores with respect to time. The polymer chains with a molecular weight of 144 kDa (**F5**) were selected to determine the stability of the polymer with different time intervals. Figure 5a shows the data obtained over 15 min (900 s) at regular intervals of 200 s (see Table 1 in the Supporting Information). There is no systematic change in diffusion coefficient with time up to 700 s. These changes occurred more than 700 s exposure to laser light could be attributed to the instability of the samples in long exposure to laser light. However, 700 s (12 min) is very good for an organic molecule, like MEH-PPV, to be stable under continuous exposure to laser light. This indicates that the polymers are stable for more than 10−12 min for FCS measurements. Further, the effect of temperature on the diffusion coefficients was investigated for the polymer sample **F5**. The data was taken at different temperatures from 30 to 80 °C (at 10 °C intervals), and the results after the MEMFCS fitting are shown in Figure 5b. The diffusion coefficients decreased with the increase in the temperature, and this trend can be attributed to the expansion of polymer chains at higher temperatures. At higher temperatures, the polymers undergo a change in conformation, and therefore, the diffusion dynamics studies were restricted to room temperature (at 30 °C). Figure 5c shows the data at various concentrations of polymer samples. It was found that the concentrations in the range 10−20 nM were appropriate for performing the experiments. On the basis of the above analysis for **F5**, we used the concentration of 10 nM and a measurement time of 100 s for studying the diffusion dynamics at 30 °C.

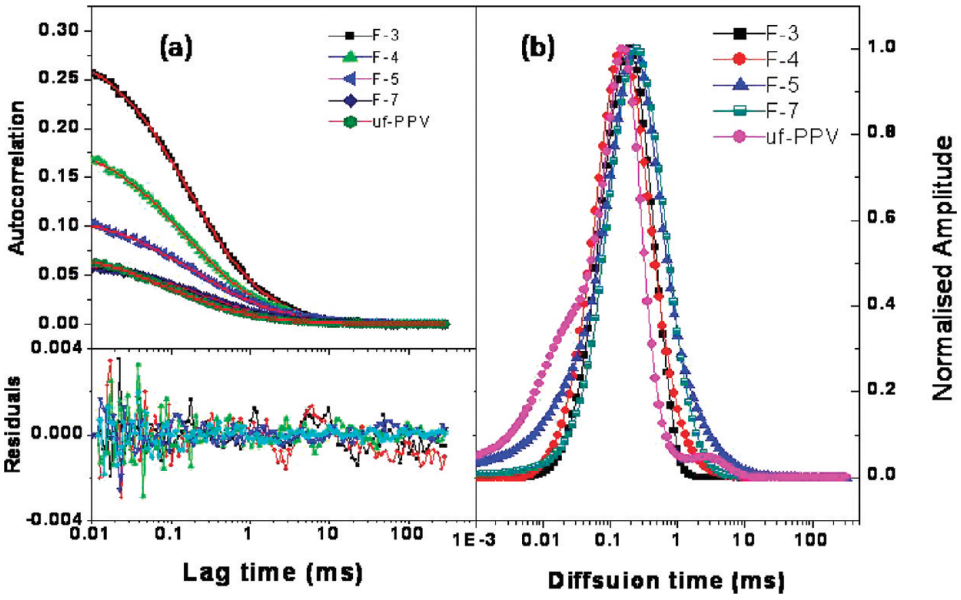


**Figure 6.** Autocorrelation curves of different molecular weight fractions (a) and their MEMFCS fits (b).

**Table 2. Molecular Weight, Diffusion Time, Diffusion Coefficient, *N*, and AFM Image Data**

| sample | $M_n$[a] (kDa) | $\tau_D$ peak[b] (ms) | $D_{fwhm}$[c] (ms) | $N = 1/G(0)$[d] | diffusion coefficient[e] ($D$, $\mu m^2/s$) | average size of the aggregates[f] (nm) |
|---|---|---|---|---|---|---|
| **F3** | 386000 | $0.190 \pm 0.03$ | 0.415 | 3.89 | 75.3 | $130 \pm 30$ |
| **F4** | 231000 | $0.147 \pm 0.01$ | 0.448 | 5.90 | 88.8 | $120 \pm 30$ |
| **F5** | 144000 | $0.190 \pm 0.01$ | 0.566 | 9.20 | 68.2 | $940 \pm 130$ |
| **F7** | 52000 | $0.246 \pm 0.02$ | 0.692 | 17.40 | 57.6 | $640 \pm 140$ |
| **uf-PPV** | 38700 | 0.147 | 0.280 | 15.86 | 96.8 | film |

[a] $M_n$ is the number average molecular weight. [b] $\tau_D$ is the peak value of the diffusion time. [c] $D_{fwhm}$ is the full width at half-maximum of diffusion time. [d] $N$ is the average number of chromophores in the detection volume. [e] The measurement of diffusion coefficient ($D$) has a correction factor due to the possible difference in the detection volume for water and toluene. [f] Average size of polymer chain aggregates based on AFM images.

To trace the role of $\pi$-conjugated chain length (or molecular weight) on the diffusion dynamics, four narrow dispersed fractionated samples (**F3**, **F4**, **F5**, and **F7**) having molecular weights of 386, 231, 144, and 52 kDa and the broad unfractionated sample (**uf-PPV**) were used. Diluted solutions of 10 nM of all these fractions in toluene were used to record autocorrelation curves. Figure 6 shows the autocorrelation curve and MEMFCS plot of all fractions (see also Table 2). The autocorrelation curve of **uf-PPV** showed multiple diffusion characteristics with two shoulders at $\tau_D = 0.02$ and 3.0 ms. The FCS probe volume used in this investigation gives around 40 $\mu$s of diffusion time for rhodamine 6G. Therefore, it is unlikely that the peak around 20 $\mu$s is due to the conventional diffusion of MEHPPV which has a much larger hydrodynamic radius compared to rhodamine 6G. We suspect that this peak is due to the faster cooperative diffusion as opposed to self-diffusion as reported by Zettl et al.[33d] However, further investigation is required to confirm the appearance of the shoulder in the diffusion peak. The appearance of small shoulders in **uf-PPV** may correspond to diffusion of polymer chains which are either long or short in the broad-disperse sample. All fractionated samples show a single peak with a certain fwhm. The position of the peak maximum of **uf-PPV** is almost similar to the low molecular weight fraction **F7** of 52 kDa. The full width at half maxima ($D_{fwhm}$, $D$ = diffusion time) of the diffusion plots were also determined (see Table 2). $D_{fwhm}$ is the measure of the diffusion distribution of chains in the sample which is similar to that of the polymer chain distribution ($R_{fwhm}$) obtained by SEC retention time (see Figure 2). The comparison of the SEC plot of **uf-PPV** (see Figure 2a) with their FCS diffusion plots (see Figure 6b) clearly indicates that the highly polydisperse sample showed multiple diffusion coefficients in the FCS data. The average number of particles or chains ($N$) in the excitation volume is determined from the inverse of $G(0)$. $D_{fwhm}$, diffusion coefficient, and "$N$" are plotted against the polymer chain length (or molecular weight) and shown in Figure 7. $D_{fwhm}$ decreases with increasing molecular weight. The average number of emissive chromophores appearing in the excitation volume ($N$) decreased with the increase in the molecular weight of the chains (see Figure 7a and b). Unlike small fluorescent molecules, in the conjugated polymers, the concentrations of the species are typically calculated on the basis of the repeating unit mass of the chromophores. Thus, for a given concentration, higher molecular weight polymers have fewer chains in solution compared to the lower molecular weight counterpart. Therefore, the increase in the $N$ values for the lower molecular weight fractions is the consequence of a greater number of short chains appearing in the detection volume (see Figure 7a). The diffusion coefficient increases with an increase in the molecular weight of the chains. This means the higher molecular weight chains (longer chain) diffuse much faster than shorter ones (see Figure 7c). At very


dx.doi.org/10.1021/jp203978v |J. Phys. Chem. B 2011, 115, 10779–10788

large molecular weights (such as **F3**), the diffusion coefficient attains a plateau which could be attributed to a limitation of FCS for very high molecular weight polymers. The diffusion coefficients have a correlation factor due to the change in detection volume. However, the trend of change in diffusion coefficient with respect to $M_n$ remains unchanged. The comparison of the data of $D_{fwhm}$, diffusion coefficient, and "$N$" of the unfractionated sample **uf-PPV** with narrow fractionated samples revealed the following points (see also Table 2): (i) the diffusion coefficients of the **uf-PPV** chains are almost similar to those of the high molecular weight polymer chains of $M_n$ = 400 kDa (**F3**) and (ii) the average number of fluorophores in the focal volume ($N$) for **uf-PPV** is very close to that of the low molecular weight chains of $M_n$ = 52 kDa (**F7**). These results of **uf-PPV** are in contradiction with the observation in the narrow dispersed samples. This indicates that the diffusion is not uniform in the unfractionated samples and their diffusion coefficient is predominantly determined by the longer chains present in the broad distribution (see Figure 2a). Therefore, it is clearly evident that FCS data for the unfractionated samples alone is not enough to establish the correlation between the molecular weight of the chains with their diffusion dynamics. It is important to fractionate the samples in order to obtain the correct diffusion coefficients using the MEMFCS algorithm. The trends in Figure 7 indicate that the diffusion dynamics of the chains is predominantly influenced by the chain length rather than molecular weight distribution. All the fractions have identical chemical structure with trans-vinylene linkage; as a result, the polymer chains in the fractions are expected to have a stiff backbone structure. The number average molecular weights of the fractions have a minimum of 30 kDa, and it accounts for at least 100 repeating units in the backbone. Typical persistence lengths for the polymer are constituted by 8−10 repeating units. Therefore, the chain lengths of fractionated samples are much longer than that of the expected persistence length for MEH-PPV chains. Further, toluene is a very good and highly preferred solvent for MEH-PPV chains and it keeps the chain in the most expanded conformation.[30] Therefore, the difference in the diffusion dynamics of the polymer chains having different molecular weights is a consequence of the molecular aggregation phenomenon rather than other structural parameters like persistence length.

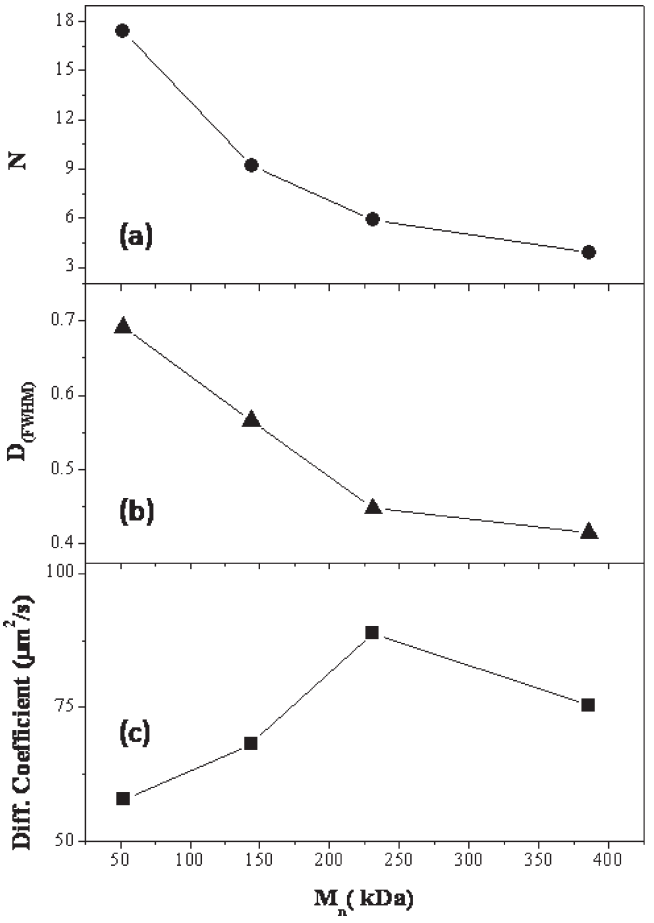


**Figure 7.** Plots of $N$ (a), $D_{fwhm}$ (b), and diffusion coefficient (c) versus $M_n$.

In order to understand the chain length dependent diffusion dynamics, the fractionated samples were subjected to AFM analysis. Typically, polymer chains exist either as expanded or collapsed globular particles in solution depending on their chain length (or molecular weight).[41] At higher molecular weight, the strong intrachain interactions result in the formation of globular (or tightly packed) particles.[42] On the other hand, lower molecular weight chains have hairy structures (like in the expanded conformation) and possess a high possibility for interchain

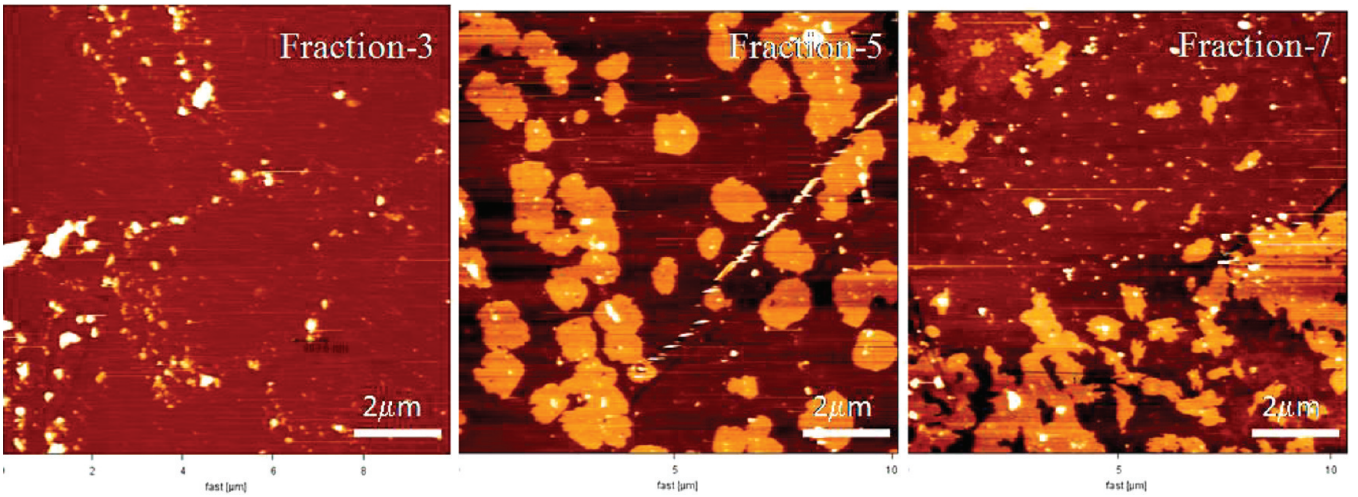


**Figure 8.** AFM images of fractionated samples.

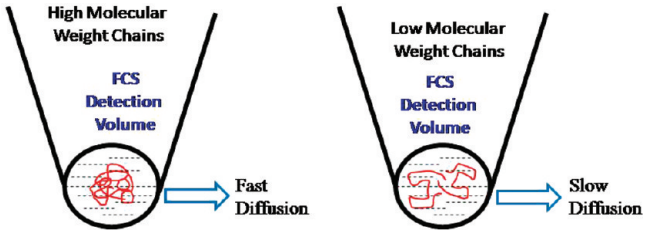


**Figure 9.** Model for diffusion of different molecular weight polymer chains at the detection volume.

interactions. Among the various available techniques to analyze the existence of chain interactions and their particulate nature, AFM images of the films cast from the dilute solutions are highly reliable. AFM images of samples **F3**, **F5**, and **F7** are shown in Figure 8. Evaporation of solvent molecules from a drop of polymer solution increases the local concentration of the polymer chains and promotes their chain interactions. Strong intrachain interactions produce tiny particles, whereas larger particles are produced via interchain interactions. Higher molecular weight sample **F3** produced 130 nm tiny particles, whereas micrometer sized larger particles were formed by **F5**. For very low molecular weight polymers (in the sample **F7**), the particulate nature is lost and it appeared as a film via strong interchain interactions. The size of the structures formed in the dilute solutions inferred from the hydrodynamic radius in FCS data is much smaller compared to the aggregates in AFM images. This is because AFM images are taken after the aggregates settled down after evaporation of solvents. It should be noted that the AFM shows smaller aggregates for longer chains compared to shorter chains, indicating the beginning of aggregation and interchain interactions in the solution itself. On the basis of the above experimental evidence, a model has been proposed for the diffusion dynamics of the conjugated polymers in solution in Figure 9. There are two important factors that affect the mobility of the chains in dilute solutions: (i) the size of the polymer chain aggregates (or particles) and (ii) the interparticle interactions. In a dilute solution, the globular tiny molecules move fast and have relatively less probability for the interparticle interactions. Low molecular weight chains possessed hairy structures, which inherently enhance the interparticle interaction. As a consequence, the diffusion became slow in the low molecular weight chains. Hence, the larger polymer chain lengths experience fast diffusion in solution compared to their low molecular weight counterparts. In a nutshell, in the present investigation, we have clearly proved that the isolation of narrow polydisperse conjugated sample is very much crucial in establishing the correlation between diffusion dynamics and chain length (or molecular weights) of $\pi$-conjugated polymers using FCS.

## CONCLUSIONS

In conclusion, the diffusion dynamics of the $\pi$-conjugated polymer was investigated for freshly synthesized and narrow molecular fractionated MEHPPV using FCS. The important outcome of the present investigation may be summarized as follows: (i) narrow polydispersed samples of molecular weights ranging from 500 to 20 kDa were obtained by the fractionation techniques, (ii) the retention time based $R_{fwhm}$ of SEC chromatogram is found to be a more suitable representation for the distribution of the fractionated samples, (iii) the photophysical properties of the fractionated samples are almost identical for the entire molecular weight range of 500 to 20 kDa, (iv) the maximum entropy based fitting (MEMFCS) method is used to determine the diffusion time from the FCS data and this method is particularly useful in such situations where the diffusion dynamics is strongly heterogeneous, (v) three parameters obtained from FCS such as $D_{fwhm}$, diffusion coefficient, and average number of particles in excitation volume ($N$) are used to trace the diffusion dynamics of the polymer chain, (vi) $D_{fwhm}$ and $N$ decrease with the increase in the molecular weight of the chains, whereas the diffusion coefficient showed the opposite trend, (vii) AFM studies revealed the formation of tiny nanoparticles at higher molecular chains, and (viii) the high molecular weight chains possessed globular structure and diffused faster in solution, whereas the low molecular weight chains possessed interparticle interaction and show slow diffusion in solution. The approach demonstrated here may be very useful for establishing the role of the $\pi$-conjugated chain length (or molecular weight) while processing them from dilute solution in electronic devices such as light emitting diodes and photovoltaics.

## ASSOCIATED CONTENT

**Supporting Information.** Table for the diffusion time and diffusion coefficients of fraction F5 at various time intervals, temperatures, and concentrations, a picture of a home-built fluorescence correlation spectroscope, the autocorrelation curve of rhodamine 6G in water, an AFM image, decay profiles of all the polymer samples, $^{1}H$ and $^{13}C$ spectra of monomer and polymer samples, plots of molecular weights and distribution, and plots of quantum yields and absorbance maxima versus molecular weight. This material is available free of charge via the Internet at http://pubs.acs.org.

## AUTHOR INFORMATION

### Corresponding Author

*E-mail: s.patil@iiserpune.ac.in (S.P.); jayakannan@iiserpune.ac.in (M.J.).

## ACKNOWLEDGMENT

We thank Department of Science of Technology, New Delhi, India, for financial support under the NSTI Programme SR-NM/NS-42/2009 and SR-NM/NS-84/2009. We also thank department of information technology for financial support and help from Professor Maiti's group at TIFR-Mumbai for building the FCS setup. A.V.R.M. thanks IISER-Pune for a research fellowship, and M.G. thanks CSIR, New Delhi, India, for a research fellowship.

## REFERENCES

(1) Burroughes, J. H.; Bradley, D. D. C.; Brown, A. R.; Marks, R. N.; Mackay, K.; Friend, R. H.; Burns, P. L.; Holmes, A. B. *Nature* **1990**, *347*, 539–541.

(2) Friend, R. H.; Gymer, R. W.; Holmes, A. B.; Burrouges, J. H.; Marks, R. N.; Taliani, C.; Bradley, D. D. C.; Dos Santos, D. A.; Gredas, J. L.; Longlund, M.; et al. *Nature* **1999**, *397*, 121–128.

(3) Sheats, J. R.; Antoniadis, H.; Hueschen, M.; Leonard, W.; Miller, J.; Moon, R.; Roitman, D.; Stocking, A. *Science* **1996**, *273*, 884–888.

(4) Kraft, A.; Grimsdale, A. C.; Holmes, A. B. *Angew. Chem., Int. Ed.* **1998**, *37*, 402–408.

(5) Traiphol, R.; Charoenthai, N.; Srikhirin, T.; Kerdcharoen, T.; Osotchan, T.; Maturos, T. *Polymer* **2007**, *48*, 813–826.
(6) Hsu, J. H.; Fann, W.; Tsao, P. H.; Chuang, K. R.; Chen, S. A. *J. Phys. Chem. A* **1999**, *103*, 2375–2380.
(7) Jakubiak, R.; Collison, C. J.; Wan, W. C.; Rothberg, L. J.; Hsieh, B. R. *J. Phys. Chem. A* **1999**, *103*, 2394–2398.
(8) Chen, S. H.; Su, A. C.; Chou, H. L.; Peng, K. Y.; Chen, S. A. *Macromolecules* **2004**, *37*, 167–173.
(9) Huang, W. Y.; Matsuoka, S.; Kwei, T. K.; Okamoto, Y. *Macromolecules* **2001**, *34*, 7166–7171.
(10) Setayesh, S.; Grimsdale, A. C.; Weil, T.; Enkelmann, V.; Mullen, K.; Meghdadi, F.; List, E. J. W.; Leising, G. *J. Am. Chem. Soc.* **2001**, *123*, 946–953.
(11) Becker, H.; Spreitzer, H.; Kreuder, W.; Kluge, E.; Schenk, H.; Parker, I.; Cao, Y. *Adv. Mater.* **2000**, *12*, 42–48.
(12) Nguyen, T. Q.; Doan, V.; Schwartz, B. J. J *Chem. Phys.* **1999**, *110*, 4068–4078.
(13) Cyriac, A.; Amrutha, S. R.; Jayakannan, M. *J. Polym. Sci., Polym. Chem.* **2008**, *46*, 3241–3256.
(14) Padmanabhan, G.; Ramakrishnan, S. *J. Am. Chem. Soc.* **2000**, *122*, 2244–2251.
(15) Liao, L.; Pang, Y.; Ding, L.; Karasz, F. E.; Smith, P. R.; Meador, M. A. *J. Polym. Sci., Polym. Chem.* **2004**, *42*, 5853–5862.
(16) (a) Liao, L.; Pang, Y.; Ding, L.; Karasz, F. E. *Macromolecules* **2002**, *35*, 3819–3824. (b) Pang, Y.; Li, J.; Hu, B.; Karasz, F. E. *Macromolecules* **1999**, *32*, 3946–3950.
(17) Liao, L.; Pang, Y.; Ding, L.; Karasz, F. E. *Macromolecules* **2001**, *34*, 6756–6760.
(18) Zheng, M.; Sarker, A. M.; Gurel, E. E.; Lahti, P. M.; Karaz, F. E. *Macromolecules* **2000**, *33*, 7426–7430.
(19) (a) Chou, C. H.; Hsu, S. L.; Dinakaran, K.; Chiu, M. Y.; Wei, K. H. *Macromolecules* **2005**, *38*, 745–751. (b) Xia, C.; Advincula, R. C. *Macromolecules* **2001**, *34*, 5854–5859.
(20) (a) Yang, J. S.; Swager, T. M. *J. Am. Chem. Soc.* **1998**, *120*, 5321–5322. (b) Yang, J. S.; Swager, T. M. *J. Am. Chem. Soc.* **1998**, *120*, 11864–11873.
(21) Wang, H.; Song, N.; Li, H.; Li, Y.; Li, X. *Synth. Met.* **2005**, *151*, 279–284.
(22) Tang, R.; Chuai, Y.; Cheng, C.; Xi, F.; Zou, D. *J. Polym. Sci., Part A: Polym. Chem.* **2005**, *43*, 3126–3140.
(23) Bao, Z.; Amundson, K. R.; Lovinger, A. J. *Macromolecules* **1998**, *31*, 8647–8649.
(24) Akcelrud, L. *Prog. Polym. Sci.* **2003**, *28*, 875–962.
(25) Amrutha, S. R.; Jayakannan, M. *J. Phys. Chem. B* **2006**, *110*, 4083–4091.
(26) Amrutha, S. R.; Jayakannan, M. *Macromolecules* **2007**, *40*, 2380–2391.
(27) Resmi, R.; Amrutha, S. R.; Jayakannan, M. *J. Polym. Sci., Polym. Chem.* **2009**, *47*, 2631–2646.
(28) Amrutha, S. R.; Jayakannan, M. *J. Phys. Chem. B* **2009**, *113*, 5083–5091.
(29) Goel, M.; Jayakannan, M. *J. Phys. Chem. B* **2010**, *114*, 12508–12519.
(30) Amrutha, S. R.; Jayakannan, M. *J. Phys. Chem. B* **2008**, *112*, 1119–1129 and references cited therein.
(31) (a) Krichevsky, O.; Bonnet, G. *Rep. Prog. Phys.* **2002**, *65*, 251–297. (b) Dong, C.; Qian, H.; Fang, N.; Ren, J. *J. Phys. Chem. B* **2006**, *110*, 11069–11075. (c) Chmyrov, A.; Sandén, T.; Widengren, J. *J. Phys. Chem. B* **2010**, *114*, 11282–11291. (d) Chiantia, S.; Kahya, N.; Schwille, P. *Langmuir* **2007**, *23*, 7659–7665.
(32) Magde, D.; Elson, E.; Webb, W. *Phys. Rev. Letts.* **1972**, *29*, 705–707.
(33) (a) Magde, D.; Elson, E. *Biopolymers* **1974**, *13*, 1–27. (b) Fatin-Rouge, N.; Wilkinson, K. J.; Buffle, J. *J. Phys. Chem. B* **2006**, *110*, 20133–20142. (c) Torres, T.; Levitus, M. *J. Phys. Chem. B* **2007**, *111*, 7392–7400. (d) Zettl, U.; Hoffmann, S. T.; Koberling, F.; Krausch, G.; Enderlein, J.; Harnau, L.; Ballauff, M. *Macromolecules* **2009**, *42*, 9537–9547.
(34) Lin, H.; Person, G.; et al. *Nano Lett.* **2009**, *9*, 4456–4461.
(35) Summers, M. A.; Robinson, M. R.; Bazan, G. C.; Buratto, S. K. *Chem. Phy. Lett.* **2002**, *364*, 542–546.
(36) Neef, C. J.; Ferraris, J. P. *Macromolecules* **2000**, *33*, 2311–2314.
(37) Sengupta, P.; Balaji, J.; Maiti, S. *Methods* **2002**, *27*, 374–387.
(38) Sengupta, P.; Garai, K.; Balaji, J.; Periasamy, N.; Maiti, S. *Biophys. J.* **2003**, *84*, 1977–1984.
(39) Fu, L.; Ferreira, R. A. S.; Silva, N. J. O.; Fernandes, A. J.; Ribeiro-Claro, P.; Goncalves, I. S.; Bermudez, V. Z.; Carlos, L. D. *J. Mater. Chem.* **2005**, *15*, 3117–3125.
(40) Fakis, M.; Anestopoulos, D.; Giannetas, V.; Persephonis, P. *J. Phys. Chem. B* **2006**, *110*, 24897–24902.
(41) Odian, G. *Principles of polymerization*, 4th ed.; John Wiley & Sons: India, 2007.
(42) Wang, P. S.; Lu, H. H.; Liu, C. Y.; Show, A. C. *Macromolecules* **2008**, *41*, 6500–6504.